

Measuring Higgs mass in the $H \rightarrow ZZ^* \rightarrow 4\ell$ with the ATLAS detector

Siyuan Yan on behalf of the ATLAS Collaboration^{a,*}

^aUniversity of Oxford,
Oxford, United Kingdom

E-mail: siyuan.yan@physics.ox.ac.uk

The Higgs boson mass is one of the most important free parameters in the Standard Model, and is crucial to determining the coupling strength to Standard Model particles. This is most precisely measured in the $H \rightarrow \gamma\gamma$ and $H \rightarrow ZZ^* \rightarrow 4\ell$ channels, for which the final states are fully reconstructable. This report presents a measurement for the Higgs boson mass as extracted from the four-lepton decay channel using 139 fb^{-1} of proton-proton collision data at the Large Hadron Collider by ATLAS, corresponding to the full Run 2 dataset. For a Higgs boson with $m_H = 125$ GeV, the total (stat) uncertainty is 181 MeV (178 MeV).

41st International Conference on High Energy physics - ICHEP2022
6-13 July, 2022
Bologna, Italy

*Speaker

1. Introduction

In 2012, the ATLAS and CMS collaborations announced the discovery of a neutral scalar boson, which is consistent with the Standard Model (SM) prediction of a Higgs boson. This is a major triumph for the physics programme at the Large Hadron Collider (LHC) and a significant step towards understanding electroweak symmetry breaking. The ATLAS and CMS combined measurement of the Higgs boson mass (m_H) at LHC Run1 was 125.09 ± 0.21 (stat) ± 0.11 (syst) GeV [1]. The Higgs boson mass is an important parameter to determine the coupling of the Higgs to the SM particles, including its self-coupling.

2. Lepton reconstruction and event selection

Muon is initially reconstructed independently in the Inner Detector (ID) and the Muon Spectrometer (MS). Combined tracks are reconstructed using hits from both ID and MS, and are the most common type of tracks used for ATLAS analysis involving muons as they have superior momentum resolution. A reconstructed electron consists of a cluster of energy deposits in the calorimeter and a matched ID track. Variable-size clusters are created dynamically from calorimeter-energy deposits, improving the invariant-mass resolution of the four-lepton system. Electron ID tracks are fitted using an optimised Gaussian-sum filter.

The HZZ mass measurement selects events with four isolated leptons from a common vertex and forming two pairs of oppositely charged same-flavour leptons. For each of the four channels, the first lepton pair has an invariant mass closest to the Z boson mass. The final state electrons are required to have a minimum transverse energy of 7 GeV. For reconstructed muons, the minimum transverse momentum is 5 GeV. For data, this selection is based on events collected using single-lepton, dilepton and trilepton triggers. The three higher- $(p_T$ or $E_T)$ leptons in each quadruplet are required to pass thresholds of 20, 15, and 10 GeV.

The Higgs mass resolution is improved by applying a kinematic constraint on the leading lepton pair to the Z boson mass. This methodology is referred to as the Z-mass constraint (ZMC). The inclusion of ZMC improves the resolution of $m_{4\ell}$ by 17%. The final-state radiation (FSR) photons are searched for in all events. FSR photons are found in 4% of the events and their energy is included in the mass computation, improving the resolution of $m_{4\ell}$ by 1%.

3. Signal and background model

The SM production of the Higgs boson is simulated in the next-to-next to leading order, and the major production channels include gluon fusion (ggH), vector boson fusion (VBF) and with an associated vector boson (VH). These samples are simulated for m_H between 123 to 127 GeV with 0.5 GeV intervals, and are used to reduce any residual bias in m_H in the signal modelling.

The largest source of background is non-resonant ZZ^* events, accounting for $\sim 89\%$ of the total background. This analysis floats the normalisation of the ZZ^* background. Other processes with mis-identified final states, such as Z +jets, $t\bar{t}$ and WZ processes constitute $\sim 9\%$ of the background. These processes are commonly referred to as reducible backgrounds. The residual backgrounds are tri-vector boson production, vector boson pair production in association with a top quark, and combinatorial background. These events are simulated using the PYTHIA8 generator.

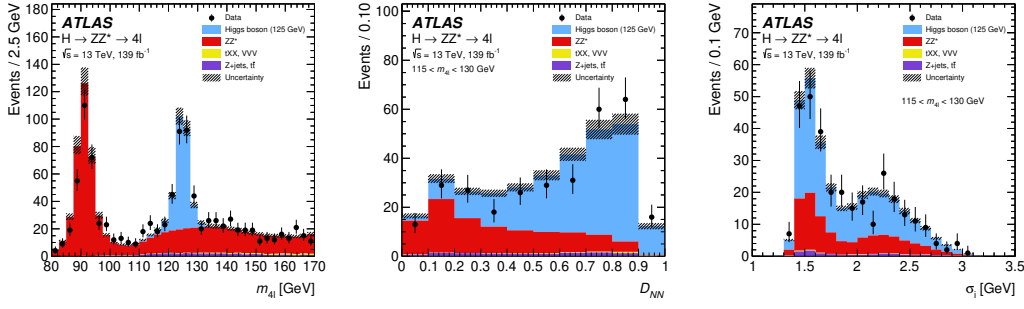


Figure 1: The observed and expected (pre-fit) $m_{4\ell}$ (left), D_{NN} (middle) and σ_i (right) distributions for the selected Higgs boson candidates. The predicted number of events for these distributions is taken from simulation for the signal, ZZ^* , tXX , and VVV processes, while it is taken from the data-driven estimate for the Z +jets and $t\bar{t}$ backgrounds. The total uncertainty in the prediction is shown by the hatched band, which also includes the theoretical uncertainties of the SM cross-section for the signal and the ZZ^* background. Higgs boson events in this plot are simulated with $m_H=125$ GeV. Taken from [2].

This signal model uses three observables, including the constrained four-lepton invariant mass ($m_{4\ell}$), the neural network discriminant for signal-background separation (D_{NN}), and the event-level $m_{4\ell}$ resolution estimate (σ_i). D_{NN} targets the separation between all Higgs production modes and the ZZ^* background. σ_i is the output of a quantile regression neural network, which targets quantile of the $|m_{4\ell}^{true} - m_{4\ell}|$ distribution. The distributions for $m_{4\ell}$, D_{NN} and σ_i are shown in Figure 1.

The signal probability density function is defined as:

$$\begin{aligned}
 P(m_{4\ell}, D, \sigma_i | m_H) &= P(m_{4\ell} | D, \sigma_i, m_H) \times P(D | \sigma_i, m_H) \times P(\sigma_i | m_H) \\
 &\approx P(m_{4\ell} | D, \sigma_i, m_H) \times P(D | m_H)
 \end{aligned}
 \tag{1}$$

For this analysis, a double-sided crystal ball (DCB) probability density function is used to model $P(m_{4\ell} | D, \sigma_i, m_H)$. The dependency on m_H is absorbed in the parametrisation of the DCB mean. With the exception of Z +jet background, 2D PDFs for the ZZ^* , $tXX + VVV$ and reducible backgrounds are constructed using simulated events for each final state. For Z +jets, data from dedicated control regions are used to reconstruct 2D Probability Density Functions (PDF). The PDFs are generated using an adaptive kernel estimation technique with Gaussian kernels to reduce fluctuations and boundary effects. The resulting probability density function is shown in Fig. 2 left for the $m_H = 125$ GeV signal sample. In the fit of the model to the data, m_H can vary freely while the other parameters are constrained to vary in accordance with the impact of the relevant systematic uncertainties.

4. Results

The final mass measurement is performed by performing a simultaneous unbinned maximum-likelihood fit to the four subchannels for $105 < m_{4\ell} < 160$ GeV. Main sources of systematic uncertainties are the electron energy scale, muon momentum scale and resolution. Other sources, including background modelling, simulation statistics and luminosity calculation, contribute to less

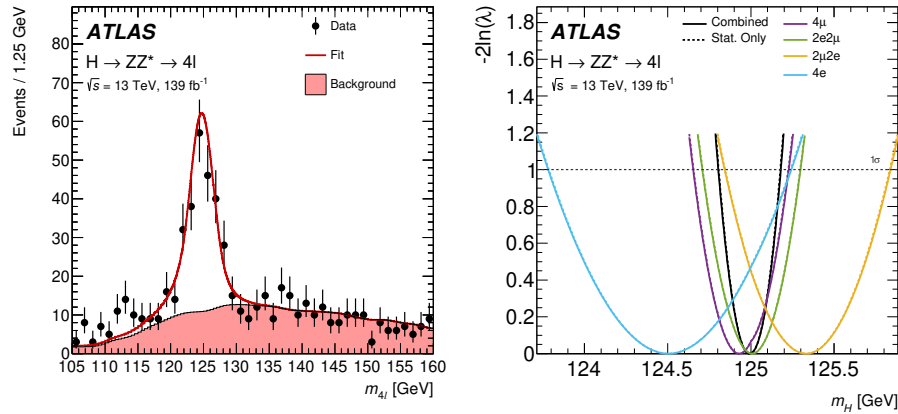


Figure 2: Left: The $m_{4\ell}$ data distribution from all subchannels combined (black points) is shown along with the signal-plus-background post-fit probability density function (red line). Right: The test statistic, $-2\ln(\lambda)$, values as a function of m_H are shown for the fit in each of the final states 4μ (purple), $2e2\mu$ (green), $2\mu2e$ (orange), and $4e$ (blue), and for the combined fit (black), both with (solid lines) and without (dashed lines) systematic uncertainties. The horizontal dashed line indicates the location of the one- σ uncertainty. Taken from [2]

than 5 MeV. The fit results in

$$m_H = 124.99 \pm 0.18(\text{stat.}) \pm 0.04(\text{syst.}) \text{ GeV.}$$

This fit is also performed independently in each channel as shown in Figure 2, with a p -value of 0.82. The result of this measurement is combined with the measurement of m_H using the Run 1 dataset in the same final states, which was $m_H = 124.51 \pm 0.52$ [3], and with a p -value of 0.4.

References

- [1] ATLAS Collaboration and CMS Collaboration. “Combined Measurement of the Higgs Boson Mass in pp Collisions at $\sqrt{s} = 7$ and 8 TeV with the ATLAS and CMS Experiments”. *Phys. Rev. Lett.* 114 (2015), p. 191803. doi: [10.1103/PhysRevLett.114.191803](https://doi.org/10.1103/PhysRevLett.114.191803).
- [2] ATLAS Collaboration. “Measurement of the Higgs boson mass in the $H \rightarrow ZZ^* \rightarrow 4\ell$ decay channel using 139 fb^{-1} of $\sqrt{s} = 13$ TeV pp collisions recorded by the ATLAS detector at the LHC” (). doi: [10.48550/arXiv.2207.00320](https://doi.org/10.48550/arXiv.2207.00320). arXiv: [2207.00320](https://arxiv.org/abs/2207.00320) [hep-ex].
- [3] ATLAS Collaboration. “Measurement of the Higgs boson mass from the $H \rightarrow \gamma\gamma$ and $H \rightarrow ZZ^* \rightarrow 4\ell$ channels in pp collisions at center-of-mass energies of 7 and 8 TeV with the ATLAS detector”. *Phys. Rev. D* 90 (2014), p. 052004. doi: [10.1103/PhysRevD.90.052004](https://doi.org/10.1103/PhysRevD.90.052004). arXiv: [1406.3827](https://arxiv.org/abs/1406.3827) [hep-ex].
- [4] D. de Florian et al. “Handbook of LHC Higgs Cross Sections: 4. Deciphering the Nature of the Higgs Sector”. 2/2017 (2016). doi: [10.23731/CYRM-2017-002](https://doi.org/10.23731/CYRM-2017-002). arXiv: [1610.07922](https://arxiv.org/abs/1610.07922) [hep-ph].